Available online at www.sciencedirect.com
SCIENCE DIRECT®
Journal of Nuclear Materials 329–333 (2004) 1072–1077
journal of nuclear materials
www.elsevier.com/locate/jnucmat

Evolution of cleared channels in neutron-irradiated pure copper as a function of tensile strain

D.J. Edwards [a,*], B.N. Singh [b]

[a] *Materials Structure and Performance Group, Pacific Northwest National Laboratory, P.O. Box 999, MSIN P8-16, Richland, WA 99352, USA*

[b] *Materials Research Department, Risø National Laboratory, DK-4000 Roskilde, Denmark*

Abstract

Tensile specimens of pure copper were neutron irradiated at ~323 K to a displacement dose of 0.3 dpa (displacement per atom). Five irradiated specimens were tensile tested at 300 K, but four of the specimens were stopped at specific strains – just before the yield point at ~90% of the macroscopic yield, at 1.5% and 5% elongation, and near the ultimate tensile strength at 14.5% elongation, with the 5th specimen tested to failure ($e_T = 22\%$). SEM and TEM characterization of the deformed specimens revealed that the plastic strain was confined primarily to the 'cleared' channels only, and that channels were present in a low number even before the macroscopic yield. New primary channels and secondary channels continued to form with increasing strain, suggesting the increase in stress was related directly to the initiation of new channels as earlier sources were exhausted.

1. Introduction

The occurrence of localized deformation via dislocation channeling in irradiated materials continues to present an interesting challenge to the fusion materials community. While this phenomenon has been known for over 40 years [1–4], until recently little progress has been made in understanding the origin of the channels and the variables that influence their formation and propagation. More recent work [5–10] has led to a re-evaluation of how channels are formed and propagate in irradiated materials, as well as in unirradiated materials. Some of the outstanding issues that remain unanswered include how to precisely relate the occurrence of the yield point to the microstructure formed during irradiation, how channels are cleared of defects and leave no dislocation debris behind, and how to account for the increase in stress when no conventional work hardening processes are evident.

As part of a broader set of experiments aimed at studying localized deformation in pure metals, a simple experiment was conducted wherein tensile tests of neutron-irradiated copper were stopped at intermediate strains. The aim of this experiment was to study the evolution of dislocation channels in an irradiated condition where a distinct yield point and some uniform plastic deformation existed. In the following report, we will present the results of this deformation experiment on irradiated copper and briefly discuss the results in terms of how channels are thought to initiate and control the stress–strain response of the material.

2. Experimental

The material used in the present investigation was thin (0.3 mm) sheet of oxygen-free high conductivity (OFHC) copper containing 10, 3, <1 and <1 ppm, respectively, of Ag, Si, Fe and Mg. The oxygen content of this copper was found to be 34 appm. Five tensile

* Corresponding author. Tel.: +1-509 376 4867; fax: +1-509 376 6308.
E-mail address: dan.edwards@pnl.gov (D.J. Edwards).

0022-3115/$ - see front matter © 2004 Elsevier B.V. All rights reserved.
doi:10.1016/j.jnucmat.2004.04.022

samples of OFHC copper were irradiated in the DR-3 reactor at Risø National Laboratory. Prior to irradiation, the OFHC copper samples were given a solution annealing treatment of 823 K for 2 h in a vacuum of 10^{-6} Torr. The resulting grain size and dislocation density were about 30 μm and $\sim 10^{12}$ m^{-2}, respectively. The tensile specimens were irradiated at 323 K to a dose level of 0.3 dpa (NRT). All specimens were irradiated at a displacement damage rate of $\sim 5\times 10^{-8}$ dpa (NRT)/s. The specimens were tensile tested at room temperature in an Instron machine at a strain rate of 1.2×10^{-3} s^{-1}. One specimen was tested to failure, one specimen loaded to ~90% of the upper yield stress, unloaded and then removed from the test fixture, and the remaining three specimens strained plastically to 1.5%, 5% or 14.5% elongation, unloaded and then removed from the tensile machine. The full tensile curve and the associated stress–strain curves for the other four samples are shown in Fig. 1.

The gage surface of the tensile samples were examined in a JEOL 840 SEM to document the slip step evolution in each strained condition. The surfaces of the samples were moderately oxidized from the solution annealing and subsequent irradiation, however, slip steps were observed in enough detail to establish the qualitative characteristics of their distribution across the gage section. Characterization of the microstructure of the various deformed samples was performed using a JEOL 2010F field emission-gun transmission electron microscope (FEG-TEM) operated in both transmission and scanning transmission mode. By virtue of the amplified contrast obtained from the STEM detector, STEM imaging proved particularly useful to observe the deformed microstructure in regions too thick for ordinary TEM imaging. For TEM specimen preparation 3-mm discs were punched from the center of the gage length of tensile specimens after the tests were stopped. These discs were twin-jet electropolished at ~293 K in a solution of 25% phosphoric acid, 25% ethylene glycol and 50% water at ~180 mA.

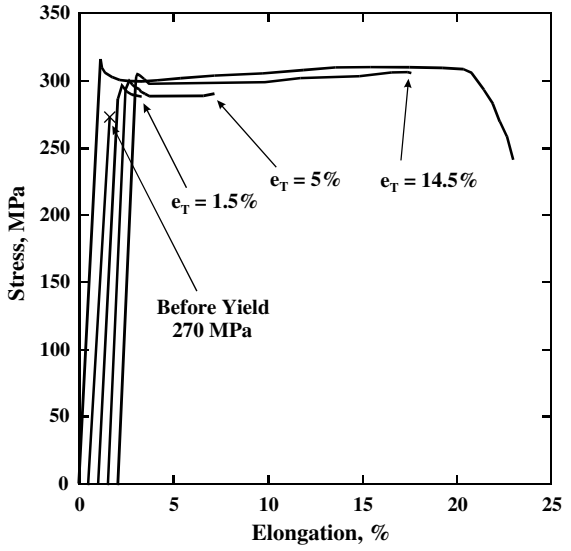

Fig. 1. The tensile curves for each of the 5 tested conditions are presented, illustrating the stress and strain at which the tests were stopped for each specimen (indicated by the arrows). Note that some variability exists from specimen to specimen, so the yield point varies slightly. The tensile curves are offset from the origin for purposes of clarity.

3. Results and discussion

For the condition where the test was stopped just before the upper yield point (~270 MPa), SEM of the gage surface of the tested sample revealed only a few isolated slip steps that had penetrated the oxide on the surface. For the specimens tested to higher strains and to failure, distinct slip steps were observed. Fig. 2 presents examples of the slip step evolution as a function of increasing plastic strain, including the slip steps observed in the necked region of the specimen tested to failure. A clear trend emerged where increasing the plastic strain produced a higher density of slip steps in a given grain, as well as activating secondary slip systems that in many cases bisected the original slip steps. Some grains possessed a higher areal density of slip steps compared to adjacent grains.

The SEM images (Fig. 2(d) and (e)) taken from the sample tested to failure revealed that the slip steps continued to increase in step height and frequency when moving into the necked region to the final point of ductile failure. This sample exhibited a significant reduction in area and failed by a ductile failure mode based on the dimples observed in the final, knife-edge failure region. The morphology of the slip steps indicated that the material was being increasingly divided into smaller, roughly rectangular blocks of material bounded by slip steps, which are believed to be correlated with individual dislocation channels based on our TEM observations. This division of the grain into discrete volumes mimics the behavior of the cell wall formation in unirradiated copper, which allows the subgrains to rotate with respect to each other and still maintain crystalline continuity by virtue of the dislocation tangles and cell walls.

TEM characterization revealed a high density ($\sim 2.5\times 10^{23}$ m^{-3}) of stacking fault tetrahedra (SFT) with a lower density ($\sim 10^{21}$ m^{-3}) of rafts of dislocation loops and dislocation segments. In the case of the sample where the test was stopped just before plastic yielding, the TEM characterization confirmed the absence of any channels on a wide scale, however, as shown in Fig. 3, isolated dislocation channels were observed in a couple

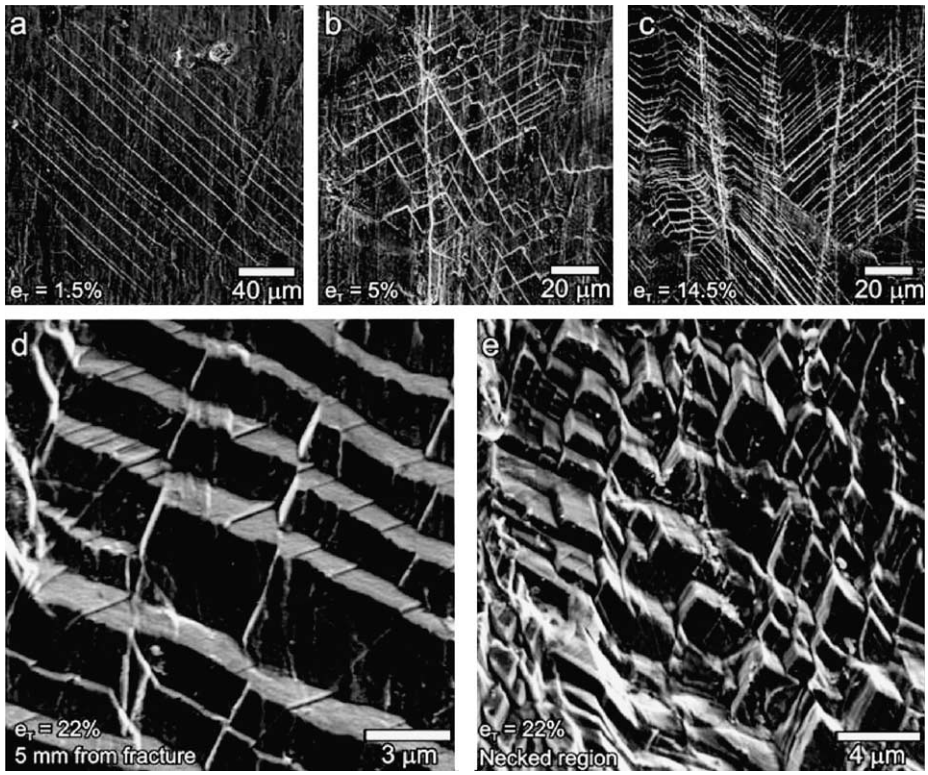

Fig. 2. Examples of the slip step evolution as a function of strain are shown. As the plastic strain increases, the density of slip steps in a given grain increases and secondary slip steps begin to arise. In the last two figures (d) and (e), the crystal has been divided into discrete rectangular volumes that appear to slide with respect to each other. The image in (d) was taken 5 mm from the final fracture, and the image in (e) was taken in the necked region less than 1 mm from the final fracture location.

of grains. In each case the channels spanned the entire grain and ended at grain boundaries. No evidence of dislocation generation was observed in the grain interiors outside the region of the few channels observed. However, it could be argued that dislocation segments have moved locally to impinge upon nearby SFT, perhaps a gradual percolation of the weakly pinned segments of a dislocation allowing it to re-stabilize under the applied load.

Surprisingly many of the grain boundaries in this latter condition appeared to have migrated during the tensile tests, leaving behind defect free zones (DFZs) of varying width. These DFZs, an example of which is shown in Fig. 3, were often observed on only one side of a grain boundary, but could cross over to the other side at a different position along the boundary or even appear on both sides. The DFZs were observed in all of the tested conditions, but at higher strains these DFZs often contained an increasing number of dislocations. They were clearly not diffusion-induced since their width was random and fluctuated along the grain boundary, and a check of the as-irradiated but untested sample did not show any such features. The same features appeared in the sample tested to failure, however the much higher level of strain tends to heavily deform the sample and obscure the DFZs because of the large plastic strains induced in these relatively soft areas.

As the strain was increased past the yield point, the TEM characterization revealed an increasing number of channels observed inside the grains, though considerable variability existed from one grain to another. The channels were generally aligned such that slip occurred along the (1 1 1) slip planes. This increase in dislocation channeling was accompanied by dislocation activity outside the channels where the dislocation segments produced during irradiation appeared to have slowly percolated through the field of SFTs. This dislocation activity did not qualitatively alter the defect population, nor produce a widespread clearing or formation of cell walls that would normally be found in unirradiated copper tested to the same strain level. At strains near the UTS it was evident that the dislocations had interacted enough to produce a tangled network of dislocations that was uniformly distributed throughout the regions in-between the channels. This type of dislocation percolation behavior in irradiated materials was observed separately in the post-irradiation annealed study of Singh et al. [10] and by Robach et al. [9] in a study of

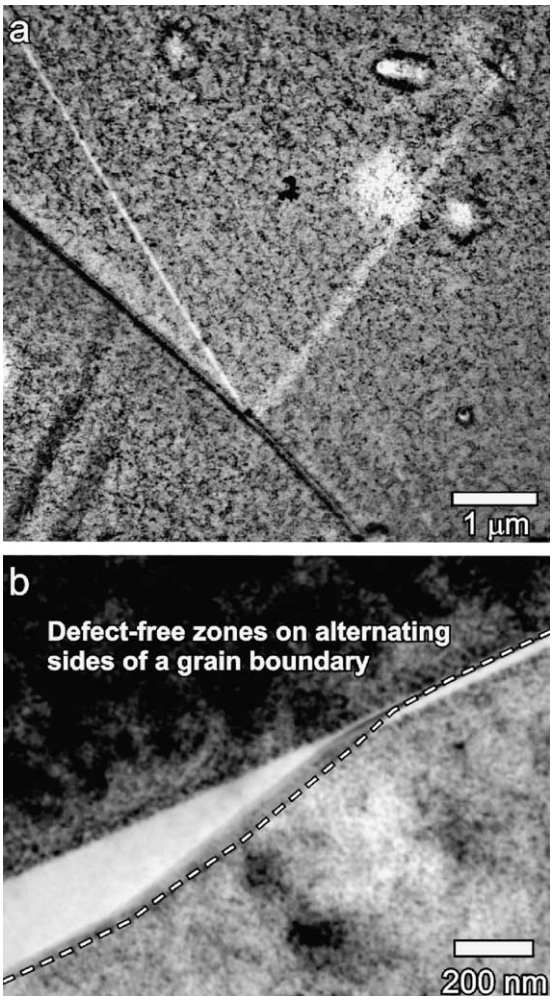

Fig. 3. Examples are shown of the microstructure in the sample loaded to ~90% of the yield stress and unloaded. A few channels such as shown in (a) spanned the entire grain, indicating that existing stress concentrations were able to initiate channels before macroscopic yield was observed in the tensile trace. The grain boundary shown in (b) is typical of the boundaries in this condition. This boundary apparently migrated during the loading and produced a defect free zone that fluctuated in width and position around the GB.

heavy-ion irradiated copper that was strained in the microscope. In the latter study they concluded that the dislocations outside the channels contributed little to the overall plasticity and that the channels were initiated from grain boundaries or crack tips.

In the sample where the test was stopped near the UTS at ~15% elongation, it was observed that new slip systems were activated inside individual grains depending on the level of strain. Fig. 4 presents evidence of these new activated slip systems. In some cases this produced larger channels indistinguishable from the channels formed earlier in the test, however, in other cases smaller, more narrow channels could be found that connected adjacent primary channels. The continued generation of new channels subdivided the crystal volume into smaller rectangular volumes similar in size to those rectangular volumes observed in the SEM slip step characterization (Fig. 2(e)). In these irradiated samples, the dislocation channels allow the discrete volumes to slide or rotate semi-independently of each other, evidence for which can be directly observed in dark field imaging and selected diffraction patterns. Instead of a uniform image, the dark field image is very complicated because discrete volumes are at slightly different orientations. This is confirmed by looking at selected area or convergent beam diffraction patterns from these localized areas, which showed that the diffraction patterns rotated and tilted from one area to the next depending on the level of strain. Note that at high strains the channels were clear of both defects and dislocations. Occasionally two or more channels intersected and produced heavy dislocation tangles, but these tangles did not extend very far into any of the channels. Because of the rarity of such dislocation tangles at channel intersections, it appears that the channels usually stopped operating before the secondary channels were activated, but this requires further confirmation.

As the strain increased it became more common to see channels intersect other channels as well as grain boundaries and annealing twins. The intersection with grain and twin boundaries often produced a noticeable shear displacement in the boundary, suggesting that some of the dislocations, or at least some component of the dislocations, were transmitted across the boundary to start a new channel in the adjacent grain. The measured displacement of the grain boundaries corresponded in some cases to as much as 40% shear strain, enough to show that hundreds of dislocations had moved through the channel. Two examples of channel intersection with boundaries are shown in Fig. 4(c) and (d). In other cases it appeared the channels did not interact with the grain boundary, however, this latter case may have arisen because the shear strain was parallel to the grain boundary at that point and produced no interaction signature. No channels were ever observed to simply start from within the grain interior unless they came from a twin boundary, interface at an inclusion, or from existing channels.

4. Conclusions

The main mode of plastic strain accumulation observed in this experiment is by dislocation channeling initiated at interfacial stress concentrations that are then able to propagate quickly through the grain, but remain confined to a narrow volume. Channels are continually

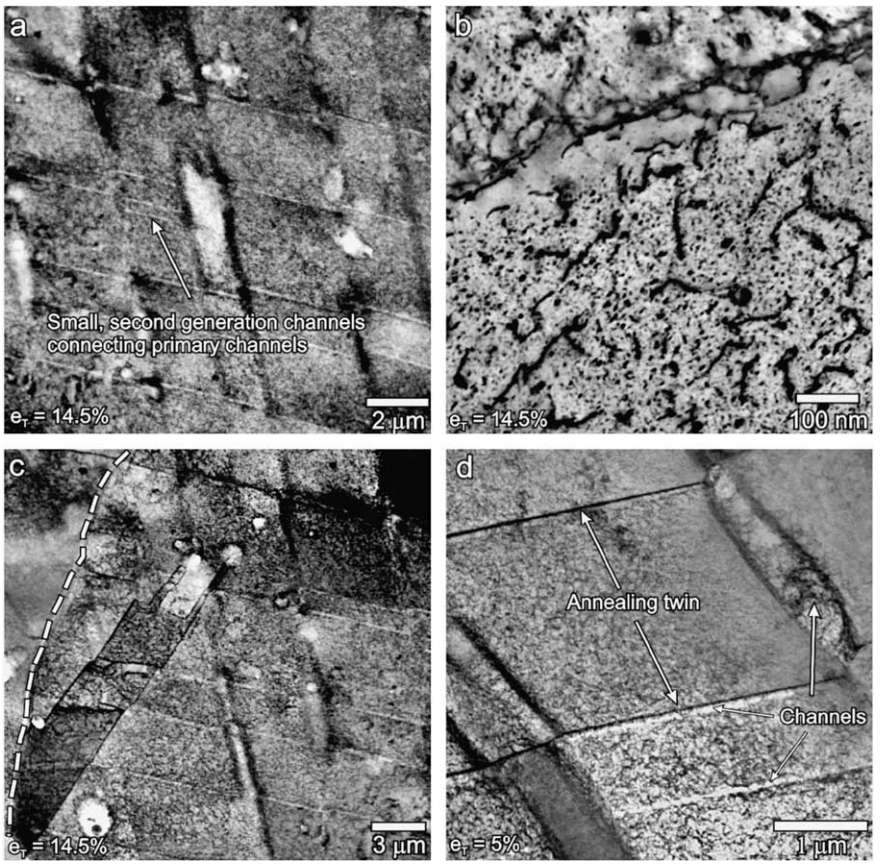

Fig. 4. Examples of shown of the increased channel density at higher strains. In the sample tested to 14.5% elongation most of the grains have some degree of channeling. The STEM image shown in (a) illustrates the different generation of channels that have formed. The TEM image in (b) shows that dislocations do move within the grain interiors, but their percolation through the SFT defects does not appear to produce a noticeable decrease in SFT density. The last two STEM images highlight examples of the interaction of channels with other channels, twin boundaries, and grain boundaries.

produced even in the necked region of the failed tensile sample, illustrating that the dense population of defects effectively inhibits the global movement of dislocations to very high plastic strains and stresses. The yield point is thought to be related to the initial generation of a isolated channels from stress concentrators (not necessarily unpinning of Frank–Read sources), which is then followed by the continual generation of new channels as the plastic strain increases to the point of necking and failure. The pre-existing dislocation segments are unable to move long distances and do not appear to play any role in channel formation. The lack of any cell wall formation or general expansion of the DFZs around grain boundaries further testifies that the dislocation segments outside of channels cannot move large distances in this irradiation condition. The continued generation of new channels past even the onset of necking subdivides the grains into smaller volumes that rotate and slide with respect to each other, much like subgrains in unirradiated and deformed copper.

Acknowledgements

The present work was partly funded by the European Fusion Technology Programme. The authors wish to thank B.F. Olsen for his technical assistance. D.J. Edwards would like to thank Risø National Laboratory for the support and assistance during his visit. His work was partly supported by the US Department of Energy under contract DE-AC06-76RLO 1830 with the Battelle Memorial Institute at the Pacific Northwest National Laboratory.

References

[1] J. Silcox, P.B. Hirsch, Philos. Mag. 4 (1959) 1356.
[2] A. Seeger, in: Proceedings of the Second UN International Conference on Peaceful Uses of Atomic Energy, Geneva, September 1958, vol. 6, p. 250.
[3] B.L. Eyre, A.F. Bartlett, Philos. Mag. 11 (1965) 53.

[4] M.J. Makin, Radiation Effects, Metallurgical Society Conference, Asheville, N.C., September 1965, in: W.F. Sheely (Ed.), AIME, vol. 37, Gordon and Breach Science Publishers, Inc., New York, 1966, p. 627.
[5] M.J. Makin, S.A. Manthorpe, Philos. Mag. 8 (1963) 1725.
[6] B.N. Singh, A.J.E. Foreman, H. Trinkaus, J. Nucl. Mater. 249 (1997) 103.
[7] M. Victoria, N. Baluc, C. Bailat, Y. Dai, M.I. Luppo, R. Schaublin, B.N. Singh, J. Nucl. Mater. 276 (2000) 114.
[8] K. Farrell, T.S. Byun, N. Hashimoto, Mapping Flow Localization Processes In Deformation Of Irradiated Reactor Structural Alloys – Final Report, ORNL/TM-2003/63, (2003).
[9] J.S. Robach, I.M. Robertson, B.D. Wirth, A. Arsenlis, Philos. Mag. 83 (8) (2003) 955.
[10] B.N. Singh, D.J. Edwards, P. Toft, J. Nucl. Mater. 299 (2001) 205.